RSC Advances

ROYAL SOCIETY OF CHEMISTRY

www.rsc.org/advances

Crystal Plane Effects of Nano-CeO_2 on its Antioxidant Activity

Yan Zhang [a], Kebin Zhou [a], Yanwu Zhai [a], Fei Qin [a], Lulu Pan [b] and Xin Yao*[a]

[a] School of Chemistry and Chemical Engineering, University of Chinese Academy of Sciences, Beijing, P. R. China.

[b] Beijing ENTE Century Environmental Technology Co., Beijing, P. R. China.

School of Chemistry and Chemical Engineering

University of the Chinese Academy of Sciences

Beijing 100049, P. R. China

*Corresponding author: Fax: +86 10 88256092; Tel: +86 10 88256980;

E-mail: yaox@ucas.ac.cn

Abstract

Due to the conflict reports on the antioxidant activity of Cerium oxide nanoparticles, much work has been done to explore the influence factors on the antioxidant activity of nano-CeO_2. However, most of the research was focused on the external factors rather than the intrinsic properties such as the exposed crystal planes of the material itself. Here we synthesized three kinds of nano-CeO_2 with different morphology by a hydrothermal process. These materials showed antioxidant ability in the following order: nanoparticles < nanobars < nanowires. The probable reason of this distinction is just due to the difference of their exposed crystal planes. Nanoparticles mainly expose the stable plane (111), while nanobars favor to expose the active plane (110) and the more active plane (100). Nanowires expose the same lattice planes as nanobars but show higher ratio of (100) / (110) due to their longer and thinner structure. The vacancy formation energy of the (100) and (110) planes is lower than that of (111) plane, the Ce^{4+} / Ce^{3+} recycle is easier for nanobars and nanowires than that for nanoparticles, resulting their better antioxidant activity. Nanowires expose higher ratio of (100) / (110), then its antioxidant activity is better than that of nanobars. This result may be helpful for further understanding of the mechanism of the antioxidant activity of nano-CeO_2.

Key words: Nanoparticles, crystal planes, antioxidant activity, electrochemical method.

Introduction

As an important rare-earth material, Cerium oxide (CeO_2) has drawn rapidly increasing attention due to its excellent activity in applications such as catalyst and fuel cell.[1-3] It also exhibits bright prospects in many biomedical treatments because of its good biocompatibility and the unique redox properties.[4] Nano-CeO_2 can prevent laser induced retinal damage, prevent cardiovascular myopathy, reduce spinal injury, and be used for detection in immunoassays and other inflammatory diseases.[5-7] On the other hand, it was also reported that CeO_2 could damage tissues by generating radicals. CeO_2 caused membrane damage to P. subcapitata, showed acute ecotoxicity to Daphnia similis at 1mg/L, induced ROS accumulation and oxidative damage to Caenorhabditis elegans and finally led to a decreased lifespan even at the exposure level of 1nM.[8-10]

In order to get a convincing explanation for the conflicts and obtain a clear and comprehensive understanding about CeO_2, much research has been done on the complex influence factors. At present, it is generally considered that the root cause for the antioxidant activity of nano-CeO_2 is its radicals scavenging function, which may derive from the redox recycle between Ce^{3+} / Ce^{4+}on the surface.[11] Therefore, the factors that affect the redox recycle may play a role on its antioxidant activity. Perez pointed out that the antioxidant properties of nano-CeO_2 are pH-dependent.[12] They supposed that a high concentration of H^+ could interfere with the regeneration of Ce^{3+}, resulting in a decrease of its antioxidant activity. It is also reported that the presence of phosphate in buffer solution alters the surface chemistry and reactivity of

nano-CeO_2 at micro-molar concentrations for Cerium phosphate formation blocks the redox recycle between Ce^{3+} / Ce^{4+}.[13]

It can be noted that most of the attention for the influence factors was focused on the externalities, however, properties of the material itself especially the morphology and exposed crystal planes attracted little attention. It is all known that the intrinsic properties of nano-CeO_2, such as the particle size, the morphology and the nature of oxygen vacancy, have a remarkable impact on its catalytic performances.[14, 15] It has been discovered that the concentration and the particle size within a certain scope have a great effect on the oxidative stress.[16] These inspire us to explore whether its other intrinsic properties would play roles on the antioxidant activity. Here we synthesized three kinds of nano-CeO_2 (nanoparticles, nanobars and nanowires) by a hydrothermal process. And then, their antioxidant activity was investigated by studying the protective effects on DNA from the hydroxyl radicals (•OH) with an electrochemical experiment. The result indicated that the antioxidant ability varied due to the distinction of their exposed crystal planes. This result may be helpful for further understanding of its antioxidant activity and to obtain CeO_2 with high antioxidant ability by regulating and controlling the morphology.

Experimental section

Reagents and instruments

Double-stranded calf thymus DNA (ds-DNA), potassium ferricyanide ($K_3[Fe(CN)_6]$), poly (dimethyldiallyl ammonium chloride) (PDDA), (2,2'-bipyridyl) dichlororuthenium(II) hexahydrate ($Ru(bpy)_3Cl_2 \cdot 6H_2O$), were purchased from

Sigma-Aldrich. Ethanol (C_2H_5OH), sodium hydroxide (NaOH), Methyl violet (MV), iron (II) sulfate heptahydrate ($FeSO_4•7H_2O$), hydrogen peroxide (H_2O_2, 30%), (hydroxymethyl) aminomethane (Tris), hydrochloric acid (HCl), hexamethylenetetramine (HMT) and cerium (III) nitrate hexahydrate ($Ce(NO_3)_3·6H_2O$) were purchased from Sinopharm Chemical Reagent Co. Ltd. (Beijing, China). Reductive gas consists of 10.1% CO and 89.9% argon. Tris-HCl buffers of different pH were prepared by adding HCl (36.5%) to Tris solution. Damage reagent H_2O_2 / Tris-HCl solution was freshly prepared by adding H_2O_2 (1mL) to Tris-HCl (9mL, 0.1M, pH 7.4); Damage reagent Fenton/Tris-HCl solutions was obtained by adding FeSO4 (0.10mL, 15mM) and H_2O_2 (1mL) to Tris-HCl (9mL, 0.1M, pH 4.7). All reagents were analytically pure and were used without further purification. Ultrapure water (18.2 MΩ·cm) was used in all experiments.

Powder X-ray diffraction (XRD) patterns of the samples were recorded on a XD-3 diffraction instrument with Cu Kα radiation (λ = 1.5406Å) purchased from Persee Co. Ltd. The Operating parameters were as follows: voltage 40kV, current 40mA, scan rate 8º/min and resolution of the scanning angle 0.02º. The surface chemistry of CeO_2 was studied using X-ray photoelectron spectroscopy (XPS). The XPS data were obtained by using an ESCA Lab220i-XL spectrometer from VG Scientific. The base pressure during XPS analysis was about 3×10^{-9} mbar, and the binding energies were referenced to the C1s line at 284.8eV from adventitious carbon. The 3d peak positions of CeO_2 were then fitted using PeakFit (version 4.0) software. Transmission electronic microscopy (TEM) images were recorded on a FEI Tecnai G2 Spirit

microscope with an accelerating voltage of 120kV, and high resolution transmission electronic microscopy (HRTEM) images were obtained on a FEI Tecnai G2 F30 S-Twin microscope at an acceleration voltage of 300kV. The special surface area of all the nanomaterials was measured by Surface Area and Pore Size Analyzer (Gemini V) with liquid nitrogen. Square-wave voltammetric detection (SWV) was performed with a CHI-440 electrochemical workstation (CH Instruments, China) with a three-electrode system. Pyrolytic graphite (PG, geometric area 0.13cm^2) disk acted as the working electrode. An Ag/AgCl (saturated KCl) electrode was used as the reference and a Pt wire served as the counter electrode. The parameters for the SWV scans were as follows: amplitude 25 mV, frequency 15 Hz, and step 4 mV. The UV-vis absorption spectrum was achieved with a UV-2550 spectrophotometer. The reducibility of the samples was valued by CO Temperature programmed reduction (TPR) method with ChemiSorb 2720 purchased from micromeritics USA.

Synthesis of nano-CeO_2

All the materials were synthesized by a hydrothermal process with little modifications.

Nanoparticles: 20mL HMT (0.125M) was added dropwise to 20mL $Ce(NO_3)_3 \cdot 6H_2O$ solution (0.025M) under continuous stirring. The mixed aqueous solution was hydrothermally treated in an autoclave (50 mL) at 150□ for 12h.[17]

Nanobars: Under the condition of stirring, 20mL $Ce(NO_3)_3$ (0.175M) was added into 20mL NaOH (4M) rapidly. After being stirred for about 20min, the suspension liquid was then transferred to an autoclave (50mL) and heated at 100□ for 10h.

Nanowires: 20mL $Ce(NO_3)_3$ (0.05M) was added into 20mL NaOH (10M) rapidly with continuous stirring. After being stirred for about 20min, the suspension liquid was then transferred to an autoclave (50mL) and heated at 100□ for 24h.[18]

All the products were washed with ultrapure water, dried at 100□ for 10h and finally calcined at 400□ for 4h in air.

Square Wave Voltammetric detection

$[Ru(bpy)_3]^{2+}$ was used for detecting the oxidization of guanine bases in DNA on the electrode by forming a greatly enhanced catalytic current.[19] For intact ds-DNA, the guanine bases are protected from the access of $[Ru(bpy)_3]^{2+}$ by the double-helix structure. However, when ds-DNA encounters damaging reagents, the shielding structure will be destroyed and, as a result, more guanine bases will exposed to $[Ru(bpy)_3]^{2+}$, leading to an increasing catalytic current.[20] If CeO_2 can protect DNA from damage by scavenging hydroxyl radical, the exposed guanine bases in DNA will be inhibited and the peak current of $[Ru(bpy)_3]^{2+}$ will decrease. By this means, the antioxidant activity of CeNPs can be detected.

In the present work, DNA was fixed on an electrode by a layer-by-layer assembly method, and then detected by SWV in a solution containing $[Ru(bpy)_3]^{2+}$. At first, the PG electrode was polished with 50nm alumina powder on a polishing cloth and successively washed and sonicated in ethanol and water. Thereafter, the electrode was modified by placing a drop of positively charged PDDA solution (30μL, 1g/L) onto it for 20min, and then washed with water and dried with a nitrogen stream. Subsequently, the same operation was taken on the electrode with a drop of negatively

charged DNA solution (30μL, 1g/L). Then the PDDA/DNA electrode was obtained, and used for SWV scans. After stabilization of the solutions for 10min, the PDDA/DNA electrodes was incubated in them with continuous stirring at 37□ for 20min, then rinsed with water and transferred to the electrochemical cell containing $[Ru(bpy)_3]^{2+}$ (50mM) for SWV detection. For DNA protection, a biocompatible single dose of CeO_2 (50nM) was used according to a literature report.[21] A suspension of CeO_2 (50μL, 10μM) was added to the DNA damage solutions mentioned above before the addition of H_2O_2, and other operations were all the same.

UV-vis photometric experiments

UV-vis absorption spectroscopy of MV can also be used to detect the ability of CeO_2 scavenging hydroxyl radical (•OH). MV has a maximum absorbance at 582 nm because of its –C=C with high density of electron cloud.[22] If •OH exists, the –C=C would be damaged, leading to a decrease of the maximum absorbance. The decrease of absorbance (denoted as ΔA) thus indirectly indicates the amount of •OH. If nano-CeO_2 can scavenge •OH, ΔA would decrease. Thus the antioxidant ability of the three kinds of materials can be reflected from the ΔA value. In order to find out whether the same regularity will show under different pH value, two solutions with different pH were adopted.

The stock suspended solutions of CeO_2 for solution B were prepared at a concentration of 10μM by being dispersed into 0.1 M Tris-HCl buffer (pH 4.7) sonicated prior to use. The reaction solution for photometric determination contained 1.2×10^{-5} M MV, 0.15mM $FeSO_4$, 1.0 M H_2O_2, 0.1 M Tris-HCl buffer (pH 4.7) and

50nM CeO_2 in a final volume of 5mL. For solution A, $FeSO_4$ is not adopted and the pH value is 7.4. After incubation for 5 min at room temperature, the absorbance of the reaction solution was measured.

Temperature programmed reduction

About 70mg CeO_2 powders were put into the middle of a glass tube carefully with silica wool blocking at both ends. And then the glass tube was heated at 300□ for an hour in the atmosphere of O_2 in order to convert the mixed valence state Ce^{3+} / Ce^{4+} into the single valence state Ce^{4+}. After cooled to room temperature, 50mg heated samples weighed exactly were transferred into a silica U-tube with some silica wool as the upholder. Then the U-tube was installed to the ChemiSorb 2720 with the temperature sensor just overhanging the samples.

After all the preparations ready, a fixed flow (25mL/min) of CO (balanced with argon) was introduced to the surface of the samples in a pre-set Temperature-programmed procedure (15 □/ min).

Results and discussion

Characterization of nano-CeO_2

From Fig. 1, typical diffraction peaks of ceria fluorite structure (JCPDS card: 34-0394) can be observed for all the samples.[23] It can be found that the peak height and the full width at half-maximum are gradually increasing according to the order: nanoparticles (curve a), nanobars (curve b) and nanowires (curve c). This tendency indicates that the particle size increased and the crystallinity becoming better as the same order according to the Debye-Scherrer formula.[24]

The special surface area of all the materials measured and the resultes shows in table 1 of support information. The surface area of nanoparticles was much smaller due to its severe aggregation as seen in the TEM images, and there is no noticable difference between nanobars and nanowires.

The size and morphology of the three kinds of nano-CeO_2 can be observed from the TEM images (Fig. 2). Nanoparticles are about 15-20nm (image A) in diameter and show obvious aggregation due to their small size. Nanobars are about 6-15nm in lateral size and 60-120nm in longitudinal (image C). Nanowires have a narrow distribution than nanobar with the average diameter about 7nm and the length around 140nm (image E), giving a higher aspect ratio of 20 than nanobars. Nanowire is thinner than that of nanobars based on the average of all the materials. TEM figure shown comparing diameter of nanobars and nanowire were shown in Fig. 1 of Support information. All the results about the diameter were in good agreement with the XRD result.

The exposed crystal planes can be studied exactly from the HRTEM images (Fig. 2). The interplanar spacing of 0.31nm (image B) indicates the dominant presence of the (111) plane for nanoparticles.[25] According to reports, the model of the rod-like structure of nano-CeO_2 is a quadrangular with two (110) planes and two (100) planes as profiles and two (110) planes as the end surface.[26] As is shown in image D, (100) plane can be found according to the interplanar 0.28nm and the lattice angle (55º) between the (111) plane and the elongation direction indicates that nanobars seem to grow along the [110] direction.[27] Thus (110) planes locate at the other two profiles

and both ends. For image F, when viewed along the [110] direction, (110) plane of nanowires can be confirmed from the lattice spacing (0.38nm) of the fringes perpendicular to the elongation direction.[28] Although exposing the same crystal planes, nanowires show higher ratio of (100) / (110) than nanobars due to their thinner and longer structure. From the above results, it can be confirmed that three kinds of nano-CeO_2 exposing different crystal planes were obtained. Thus, further study about the effect of exposed crystal planes on the antioxidant activity of CeO_2 can be carried out.

Antioxidant activity study

Square wave voltammetric (SWV) detection was adopted to study the antioxidant ability of nano-CeO_2 with different morphology, by the protection of DNA from the damage of hydroxide radical (•OH). Fig. 3A shows the antioxidant activity of nano-CeO_2 with different morphology in pH 7.4 solution. As is shown, the catalytic current increased markedly (curve b) compared with intact DNA current (curve a) after the addition of damaging agent (H_2O_2), indicating that more guanine bases exposed to $[Ru(bpy)_3]^{2+}$. That is to say, the double chain structure of DNA was damaged seriously. However, the increasing margin dropped obviously (curve c, d and e) when CeO_2 were previously added before H_2O_2. This indicated that the exposed bases were much less than that without CeO_2, which meant that all the nano-CeO_2 can protect DNA from being damaged in some degree, but the protective effect exhibited obvious difference. Nanowires showed the best antioxidant activity (curve e), and nanoparticles were the lowest (curve c). In order to prove the trend

further, the antioxidant activity of the three samples were also investigated in pH 4.7 solution and the results showed in Fig. 3B. All the samples could protect DNA by scavenging •OH and the antioxidant activity of the samples was in the same sequence with the result of that in pH 7.4 solution: nanowires (Fig. 3B curve e) > nanobars (Fig. 3B curve d) > nanoparticles (Fig. 3B curve c). Those mean that the antioxidant activity difference of all the nano-CeO_2 samples is the same in solutions with different pH value.

The antioxidant ability of the[29] nano-CeO_2 with different morphology can also be studied by comparing their ability of scavenging hydroxyl radical (•OH) with the absorption spectrum experiments of methyl violet (MV). It also proved the antioxidant activity of three samples in the same trend: nanowires > nanobars > nanoparticles. It can be noted from Fig. 4 that, comparing to the pure MV, the maximum absorbance at 582 nm decreased (curve b) when H_2O_2 was added, indicating that •OH was generated.

When CeO_2 was added before H_2O_2, ΔA reduced significantly (c, d and e), indicating nano-CeO_2 could protect MV by scavenging •OH in both solutions. The reason for the stronger protective effect in solution B than that in solution A is probably that more •OH were generated in solution B. However it can be observed from the ΔA value that the relative strength of the protective effect followed the same order: nanowires (curve e) > nanobars (curve d) > nanoparticles (curve c) in both solutions. It also demonstrated that the morphology and the exposed lattice planes of nano-CeO_2

played a great role on the ability of scavenging free radicals.

Additionally, to find out whether the morphology and crystal planes of nano-CeO_2 would change after the antioxidant process, we take nanobar as an examples to explored the morphology change by TEM and the result showed in Fig. 3 of support information. From the images we can find that the morphology and exposed planes were the same as those of the fresh materials. At the same time, all the nano-CeO_2 samples in very low concentration could persistently scavenge ·OH, also implying that its structure remain the same.

Influence factors on the antioxidant activity of nano-CeO_2

To make clear the mechanism of the morphology influence on the antioxidant activity of nano-CeO_2, all the experimental conditions were kept the same strictly, thus the distinction can only be from the material itself. It is reported that the antioxidant ability of nano-CeO_2 is related to the concentration and the particle size, and smaller particles show higher ability. In this work, all the samples were used with the same concentration (50nM), thus concentration was not the reason for the difference of the antioxidant activity. The size of nanoparticles was the smallest, but they show the lowest antioxidant activity, indicating that the size was not the key factor either. From the BET result, it can be noted that the special surface area of nanobars and nanowires was nearly the same but their antioxidant ability varied greatly, meaning that the surface area was not the dominated factor either.

Additionally, the mixed valence (Ce^{3+} / Ce^{4+}) on the surface of the nano-CeO_2 was a crucial factor for its antioxidant ability, thus XPS was used to quantify the amount of

Ce^{3+}/Ce^{4+} on the surface. Fig5 depicts the Ce3d XPS spectrogram of nano-CeO_2 with different morphology. The spectra were deconvoluted with ten peaks and the corresponding peak position was approximate for all the materials. Obvious Ce^{3+} peaks could be seen for all of the samples and Ce^{3+} amounts on the surface obtained by the Peakfit 4.0 software were: nanoparticles, 27.13%; nanobars, 25.28%; nanowires, 28.02%. It can be observed that the ratio of Ce^{3+}/Ce^{4+} showed no significant difference among the materials and were not consist with the order of their antioxidant ability. Thus it can be declared that the amount of Ce^{3+} on the surface of nano-CeO_2 was not the key factor, either.

It is generally acknowledged that the antioxidant activity of nano-CeO_2 derived from the redox recycle between Ce^{3+} and Ce^{4+} on the surface and the transformation from Ce^{4+} to Ce^{3+} is much more difficult than the counter process.[30] Thus the regeneration of Ce^{3+} might play a crucial role on the antioxidant activity of nano-CeO_2. CO Temperature programmed reduction (TPR) was employed to value the generation of Ce^{3+} on the surface of CeO_2. With the temperature increasing, Ce^{4+} was reduced to Ce^{3+} gradually from the surface to the bulk.[31] At low temperature, the process of $Ce^{4+}\rightarrow Ce^{3+}$ (regeneration of Ce^{3+}) occurred only on the surface where free radicals were scavenged in the SWV experiment. Thus the distinction of the Ce^{3+} regeneration of nano-CeO_2 with different morphology can be reflected from their TPR results at the low temperature. For the TPR curve, peak area means the amount of Ce^{4+} reduced to Ce^{3+} and the peak locates temperature indicates the difficulty degree of Ce^{4+} reduction.[32] Fig. 6 showed the TPR results at the temperature ranging from 50 □ to

250 ℃, in which the reduction of Ce^{4+} only occurred on the surface of the materials. Comparing the curve of nanowries to that of nanobars, the larger peak area means that more Ce^{3+} was produced on the surface. From the TEM result we knew that nanowires were thinner and longer than nanobars, leading to the higher specific surface area. It means that the amount of Ce^{3+} produced from Ce^{4+} on the surface is more than that of nanobars, thus a bigger peak area can be obtained for nanowires. However, for nanobars and nanoparticles, the peak area is about the same, indicating the amount of Ce^{3+} produced on the surface of nanobars (curve b) is nearly the same as that of nanoparticles (curve a). Thus, the amount of Ce^{3+} produced on the surface is not the same trend as the antioxidant activity difference. Then, it can be inferred that what decided the antioxidant activity in this experiment is not the amount of Ce^{3+} produced on the surface. For nanoparticles, the peak located at about 170 ℃ (curve a), which was higher than that of the rod-like structure (160 ℃ for nanobars (curve b) and 130 ℃ for nanowires (curve c)), indicating that it possessed the lowest reducibility. As the HRTEM result shows, the distinction of the exposed planes is intimately related to morphology of nano-CeO_2, then it could be inferred that the regeneration of Ce^{3+} on the (100) and (110) planes is much easier than that on (111) plane, which is consistent with the result of the theoretical calculation that the (100) and (110) planes are more active than (111) plane.[33] This might account for the higher antioxidant ability of the rod-like structures than nanoparticles. Some reports have also proved that nano-CeO_2 exposing (100) and (110) planes showed higher catalytic ability than that mainly exposing (111) plane.[34]

The peak of nanowires locates at about 130℃, which is much lower than that of nanobars, meaning that the regeneration of Ce^{3+} on the surface of nanowires is much easier than that of nanobars. This phenomenon should be attributed to the higher ratio of (100) / (110) on the surface of nanowires, because the regeneration of Ce^{3+} for (100) plane is easier than (110) plane.[35] This makes the recycle of Ce^{3+}/Ce^{4+} on the surface of nanowires easier, thus it can scavenge more hydroxyl radicals, leading to the higher DNA protection ability than nanobars.

Conclusion

To conclude, three kinds of nano-CeO_2 with different morphology were used to explore their antioxidant activity by a DNA protective electrochemical method. Because of the higher reactivity of (100) and (110) planes than that of (111) plane, the Ce^{4+}/Ce^{3+} recycle is much easier on the surface of nanobars and nanowires than that of nanoparticles, thus the antioxidant activity of nanobars and nanowires is better than that of nanoparticles. And for nanowires expose higher ratio of (100) / (110), it shows higher hydroxyl radical scavenging ability, resulting in a better antioxidant activity than that of nanobars. Then, in addition to external environment, the exposed crystal planes of nano-CeO_2 play a great role on the antioxidant activity, which may help us to make clear of the previous conflicting reports concerning the bio-application of nano-CeO_2 and provide guidance for their further practical application.

Acknowledgment

This work was supported by the National Nature Science Foundation of China (21271184) and the Ministry of Science and Technology of China (973 program

2014CB931900 and 2012CB932504).

References

1. X. Liu, W. Ruettinger, X. Xu and R. Farrauto, *Applied Catalysis B: Environmental*, 2005, **56**, 69-75.
2. H. Xu and X. Hou, *International Journal of Hydrogen Energy*, 2007, **32**, 4397-4401.
3. Y. Y. Tsai, W. Sigmund and K. Woan, *Future Medicine Ltd*, 2012, **5(2)**, 233-242.
4. I. Celardo, J. Z. Pedersen, E. Traversa and L. Ghibelli, *Nanoscale*, 2011, **3**, 1411-1420.
5. Ajay S. Karakoti, Sanjay Singh, *Journal of the American Chemical Society*, 2009, **131**, 14144–14145.
6. J. Chen, S. Patil, S. Seal and J. F. McGinnis, *Nature nanotechnology*, 2006, **1**, 142-150.
7. S. M. Hirst, A. S. Karakoti, R. D. Tyler, N. Sriranganathan, S. Seal and C. M. Reilly, *Small*, 2009, **5**, 2848-2856.
8. E. Artells, J. Issartel, M. Auffan, D. Borschneck, A. Thill, M. Tella, L. Brousset, J. Rose, J. Y. Bottero and A. Thiery, *PloS one*, 2013, **8**, e71260.
9. N. J. Rogers, N. M. Franklin, S. C. Apte, G. E. Batley, B. M. Angel, J. R. Lead and M. Baalousha, *Environmental Chemistry*, 2010, **7**, 50.
10. H. Zhang, X. He, Z. Zhang, P. Zhang, Y. Li, Y. Ma, Y. Kuang, Y. Zhao and Z. Chai, *Environmental science & technology*, 2011, **45**, 3725-3730.
11. Roy W. Tarnuzzer, Jimmie Colon,, *Nanoletters*, 2005, **5**, 2573-2577.
12. J. M. Perez, A. Asati, S. Nath and C. Kaittanis, *Small*, 2008, **4**, 552-556.
13. Y. Xue, Y. Zhai, K. Zhou, L. Wang, H. Tan, Q. Luan and X. Yao, *Chemistry A European Journal*, 2012, **18**, 11115-11122.
14. W. I. Hsiao, Y. S. Lin, Y. C. Chen and C. S. Lee, *Chemical Physics Letters*, 2007, **441**, 294-299.
15. L. Liu, Z. Yao, Y. Deng, F. Gao, B. Liu and L. Dong, *ChemCatChem*, 2011, **3**, 978-989.
16. J. Choi and E. Park, *Toxicology*, 2008, **245**, 90-100.
17. S. W. Du, A.I.Y. Tok, F.Y.C. Boey and W.K. Chong, *Materials Science and Engineering A*, 2007, **466**, 223-229.
18. Tana, M. Zhang, J. Li, H. Li, Y. Li and W. Shen, *Catalysis Today*, 2009, **148**, 179-183.
19. P. M. Armistead and H. H.Thorp, *Analytical Chemistry*, 2000, **72**, 3764-3770.
20. H. H. Thorp and P. M. Armistead, *Analytical Chemistry*, 2001, **73**, 558-564.
21. M. Das, S. Patil, N. Bhargava, J. F. Kang, L. M. Riedel, S. Seal and J. J. Hickman, *Biomaterials*, 2007, **28**, 1918-1925.
22. I. Carozeanu, S. Dobrinas and E. Chirila, *Talanta*, 2000, **53**, 271-275.
23. J. C. Y. Chunman Ho, *Chemical Materials*, 2005, **17**, 4514-4522.
24. V. Viswanathan, R. Filmalter, S. Patil, S. Deshpande and S. Seal, *Journal of the American Ceramic Society*, 2007, **90**, 870-877.
25. E. Aneggi, J. Llorca, M. Boaro and A. Trovarelli, *Journal of Catalysis*, 2005, **234**, 88-95.
26. K. Zhou, X. Wang, X. Sun, Q. Peng and Y. Li, *Journal of Catalysis*, 2005, **229**, 206-212.
27. N. A. M.-R and A.S. Karakoti, *Biological Materials Science*, 2008, 33-37.
28. K. I. Kenji Kaneko, *Nanoletters*, 2007, **7**, 421-425.
29. Y. Xue, Q. Luan, D. Yang, X. Yao and K. Zhou, *The Journal of Physical Chemistry C*, 2011,

115, 4433-4438.

30. G. N. Vayssilov and Annapaola Migani, *Journal of Materials Chemistry*, 2010, **20**, 10535–10546.
31. Z. L. Wu, M. J. Li and S. H. Overbury, *Journal of Catalysis*, 2012, **285**, 61-73.
32. S. Watanabe, X. L. Ma and C. S. Song, *Journal of Physical Chemistry C*, 2009, **113**, 14249-14257.
33. A. Migani, G. N. Vayssilov, S. T. Bromley, F. Illas and K. M. Neyman, *Journal of Materials Chemistry*, 2010, **20**, 10535.
34. L.D. Sun, H. X. Mai, Y.W. Zhang, W. Feng, H. P. Zhang and C. H.ua Yan, *Journal of Physical Chemistry B*, 2005.
35. X. J. Du, D. S. Zhang, L. Y. Shi, R. H. Gao and J. P. Zhang, *Journal of Physical Chemistry C*, 2012, **116**, 10009-10016.

Figure Caption

Fig. 1 XRD patterns of CeO_2: nanoparticles (a), nanorods (b), and nanowires (c)

Fig. 2 TEM images of CeO_2: nanoparticles (a), nanorods (b) and nanowires (c); HRTEM images of the corresponding materials (a', b' and c')

Fig. 3 SWV scans in pH 7.0 PBS containing $[Ru(bpy)_3]^{2+}$ (50mM) for PDDA/DNA films on a PG electrode: incubated for 20 min in Tris-HCl at pH 7.4 (A) and Fenton/Tris-HCl at pH 4.7 (B): a) without other agents, b) with H_2O_2, c) with CeO_2 nanoparticles/H_2O_2, d) with CeO_2 nanobars/H_2O_2, and e) with CeO_2 nanowires/H_2O_2.

Fig. 4 UV-vis absorption spectra of MV with different added agents in pH7.4 Tis-HCl (A): (a) MV, (b) MV/H_2O_2; (c) MV /H_2O_2 /CeO_2 nanoparticles; (d) MV /H_2O_2 /CeO_2 nanobars and (e) MV /H_2O_2 /CeO_2 nanowires; and in pH4.7 Tis-HCl (B): (a) MV, (b) MV/H_2O_2/$FeSO_4$; (c) MV / H_2O_2 /$FeSO_4$ /CeO_2 nanoparticles; (d) MV /H_2O_2/$FeSO_4$/CeO_2 nanobars and (e) MV /H_2O_2/$FeSO_4$/CeO_2 nanowires at an incubation time of 5min.

Fig. 5 Ce 3d3/2, 5/2 XPS spectra of nanoparticles(a), nanobars(b) and nanowires(c).

Fig. 6 Temperature-programmed reduction (TPR) profiles of CO: (a) CeO_2 nanoparticles, (b) CeO_2 nanorods and (c) CeO_2 nanowires.

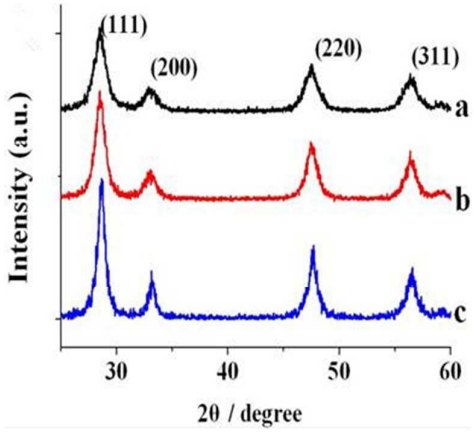

Fig. 1

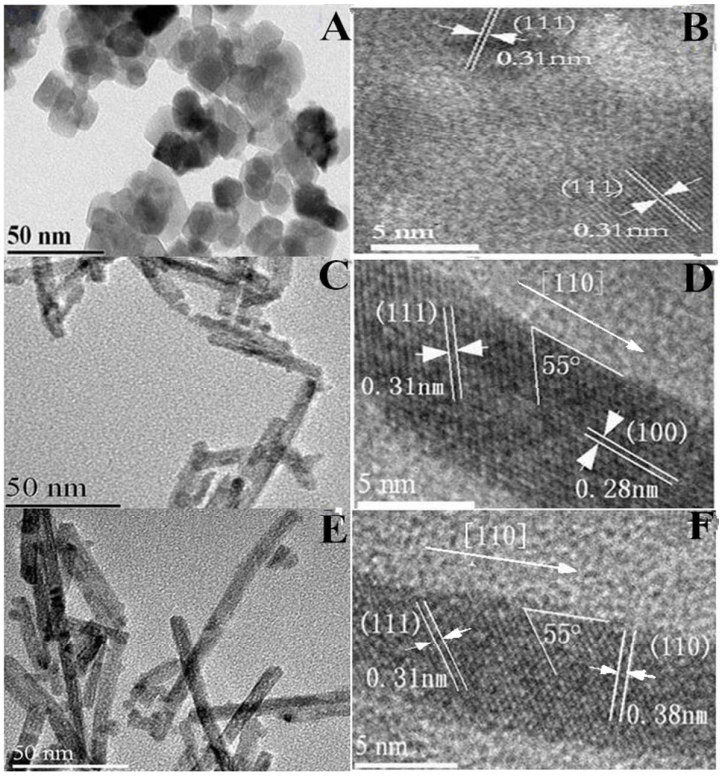

Fig. 2

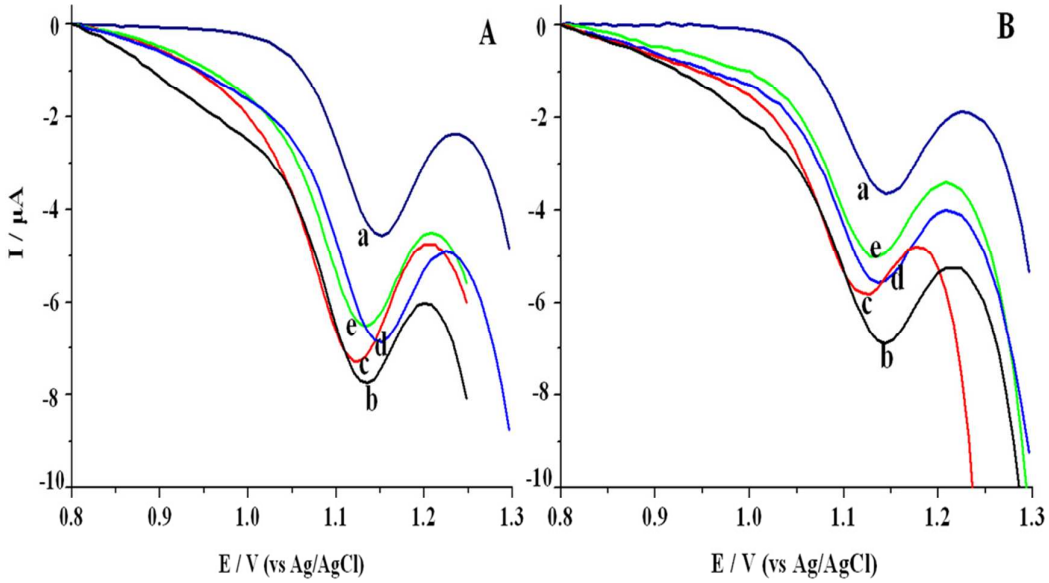

Fig. 3

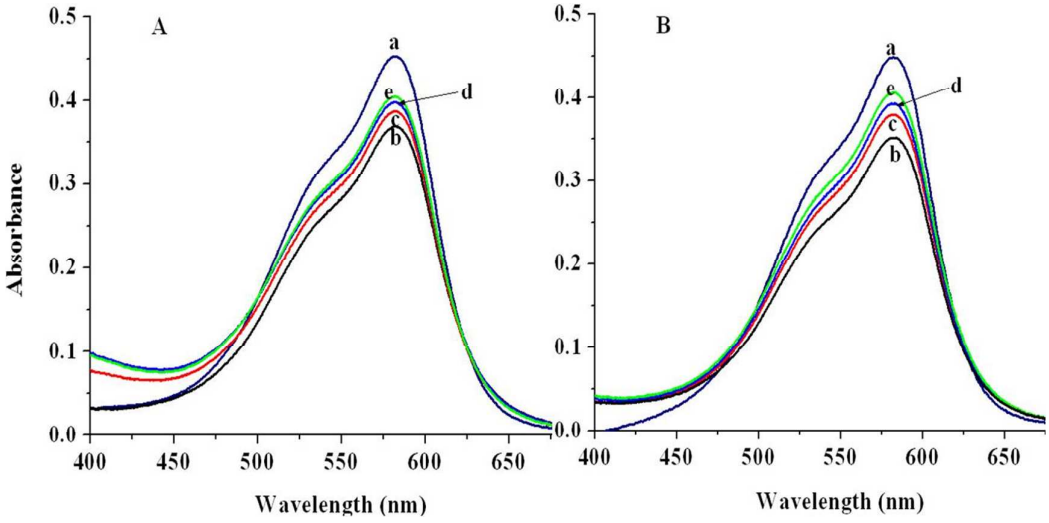

Fig. 4

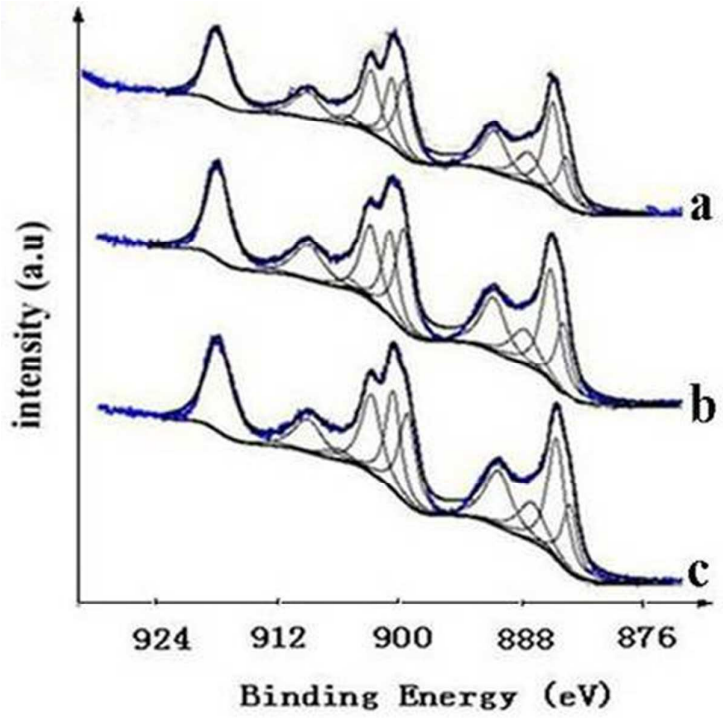

Fig. 5

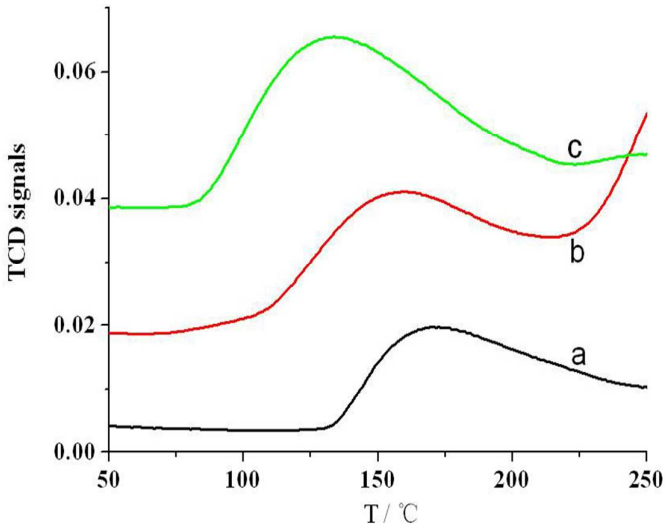

Fig. 6

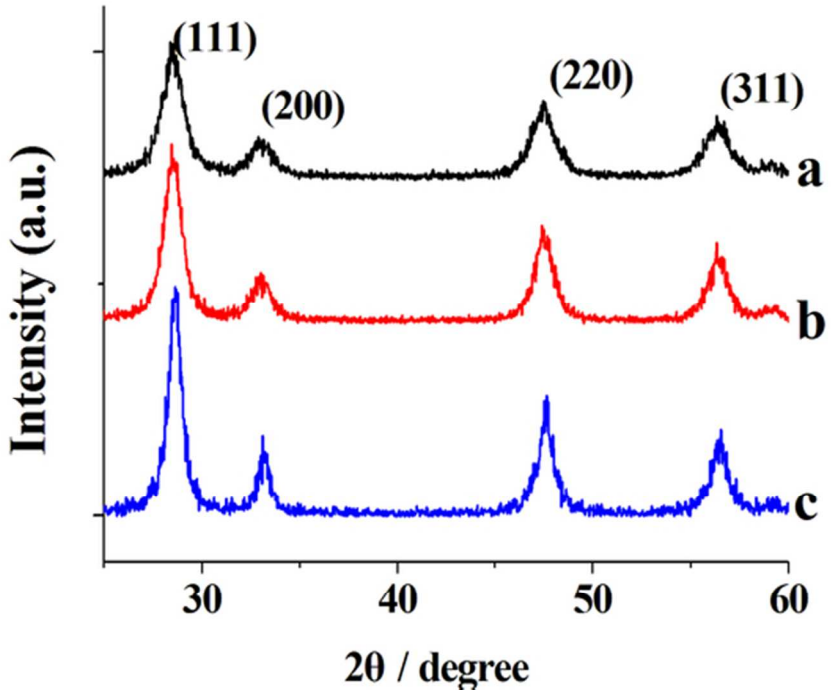

XRD patterns of CeO2: nanoparticles (a), nanorods (b), and nanowires (c)
53x41mm (300 x 300 DPI)

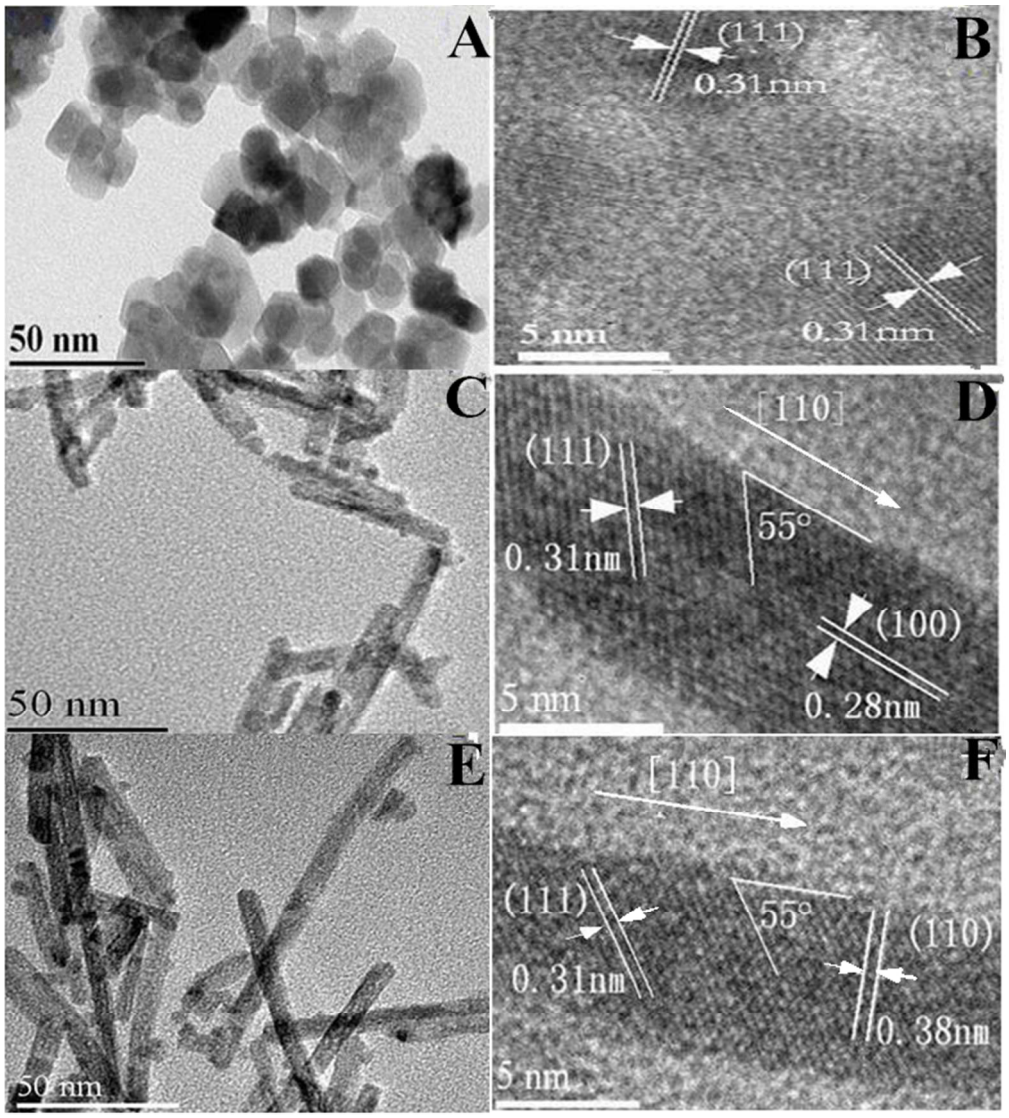

TEM images of CeO2: nanoparticles (a), nanorods (b) and nanowires (c); HRTEM images of the corresponding materials (a', b' and c')
273x302mm (72 x 72 DPI)

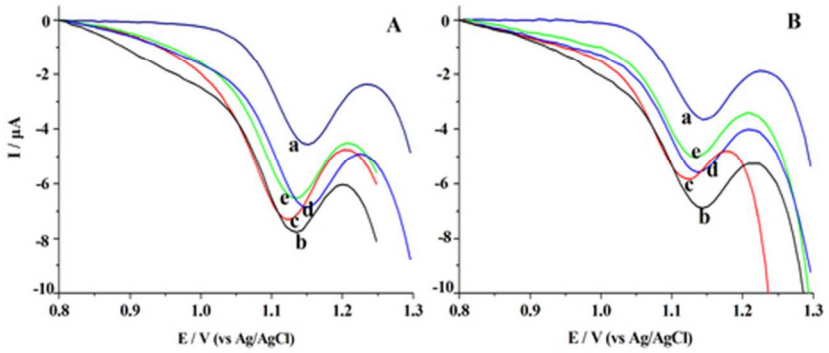

SWV scans in pH 7.0 PBS containing [Ru(bpy)3]2+ (50mM) for PDDA/DNA films on a PG electrode: incubated for 20 min in Tris-HCl at pH 7.4 (A) and Fenton/Tris-HCl at pH 4.7 (B): a) without other agents, b) with H2O2, c) with CeO2 nanoparticles/H2O2, d) with CeO2 nanobars/H2O2, and e) with CeO2 nanowires/H2O2.
53x21mm (300 x 300 DPI)

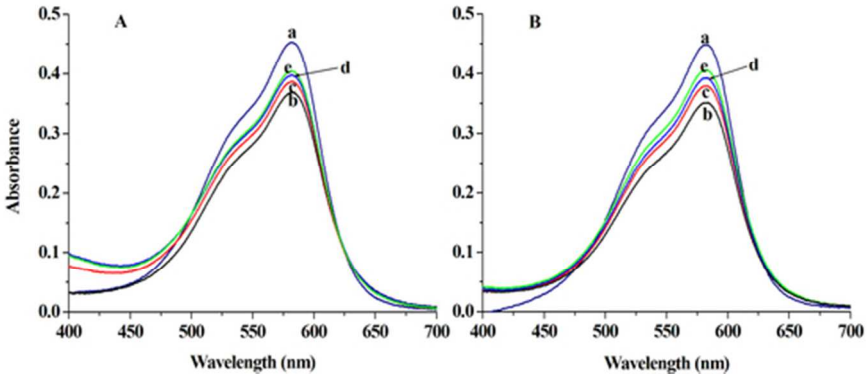

UV-vis absorption spectra of MV with different added agents in pH7.4 Tis-HCl (A): (a) MV, (b) MV/H2O2; (c) MV /H2O2 /CeO2 nanoparticles; (d) MV /H2O2 /CeO2 nanobars and (e) MV /H2O2 /CeO2 nanowires; and in pH4.7 Tis-HCl (B): (a) MV, (b) MV/H2O2/FeSO4; (c) MV / H2O2 /FeSO4 /CeO2 nanoparticles; (d) MV /H2O2/FeSO4/CeO2 nanobars and (e) MV /H2O2/FeSO4/CeO2 nanowires at an incubation time of 5min.
53x22mm (300 x 300 DPI)

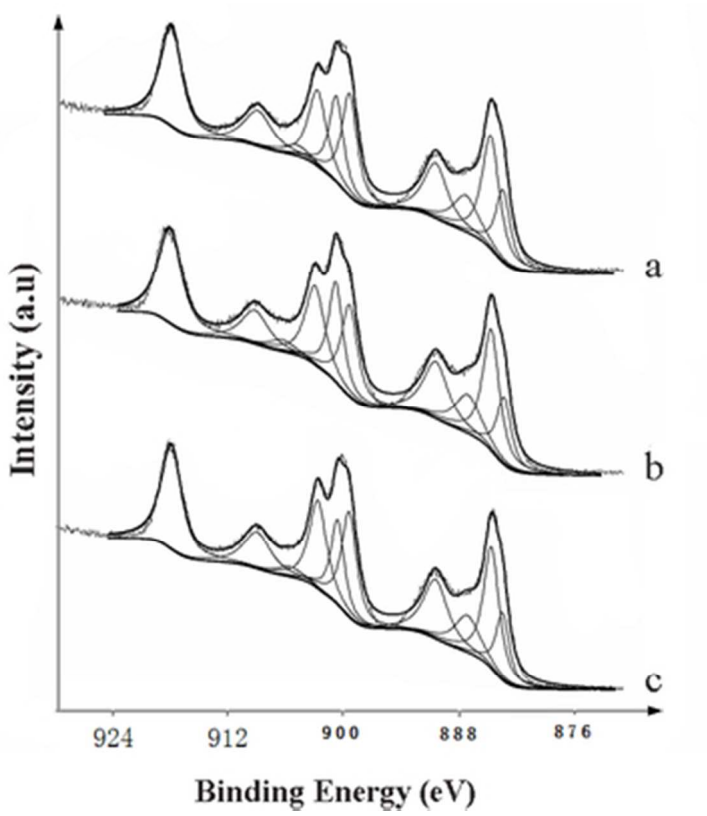

Ce 3d3/2, 5/2 XPS spectra of nanoparticles(a), nanobars(b) and nanowires(c).
30x34mm (300 x 300 DPI)

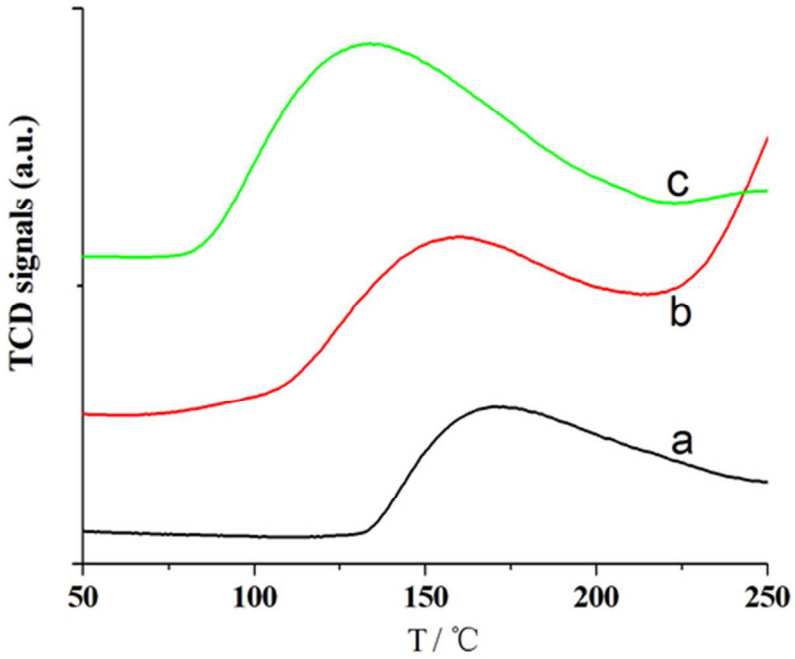

Temperature-programmed reduction (TPR) profiles of CO: (a) CeO2 nanoparticles, (b) CeO2 nanorods and (c) CeO2 nanowires.
53x41mm (300 x 300 DPI)

Graphical abstract

Crystal Plane Effects of Nanocrystalline CeO_2 on its Antioxidant Activity

Yan Zhang[a], Kebin Zhou[a], Yanwu Zhai[a], Fei Qin[a], Lulu Pan[b], and Xin Yao*[a]

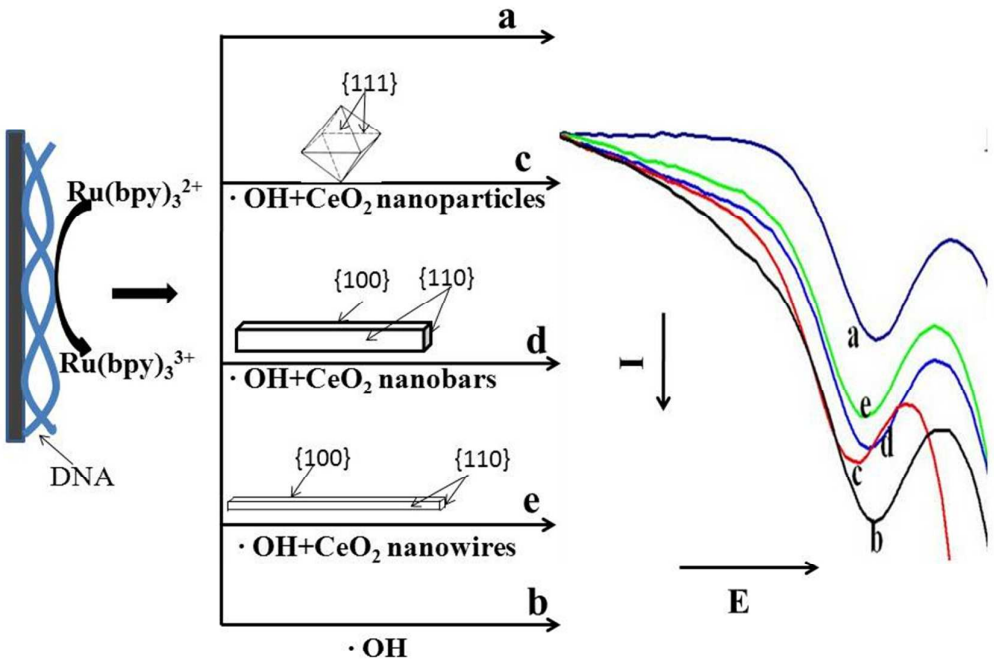

The crystal planes effect of nano-CeO_2 on its antioxidant activity was firstly investigated. By scavenging free radical, nano-CeO_2 can protect DNA from damage, but nano-CeO_2 exposing different crystal planes show different antioxidant ability. Rod-like nano-CeO_2 which expose (100) and (110) planes showed much higher antioxidant ability than nanoparticles which mainly expose (111) plane. Nanowires showed higher ability than nanobars due to the higher ratio of (100)/(110).